Study of polycarbonate-polystyrene interfaces using Scanning Transmission Electron Microscopy-Spectrum Imaging (STEM-SI)

Ruchi Pal[a1], Arun K. Sikder[b], Kei Saito[c2], Alison M. Funston[c,d] and Jayesh R. Bellare[e]

[a]IITB-Monash Research Academy, IIT Bombay, Mumbai 400076, India

[b]SABIC Research and Technology Pvt. Ltd., Bengaluru 562125, India

[c]School of Chemistry, Monash University, Clayton, Victoria 3800, Australia

[d]ARC Centre of Excellence in Exciton Science, School of Chemistry, Monash University, Clayton, Victoria 3800, Australia

[e]Department of Chemical Engineering, IIT Bombay, Mumbai 400076, India.

Graphical Abstract

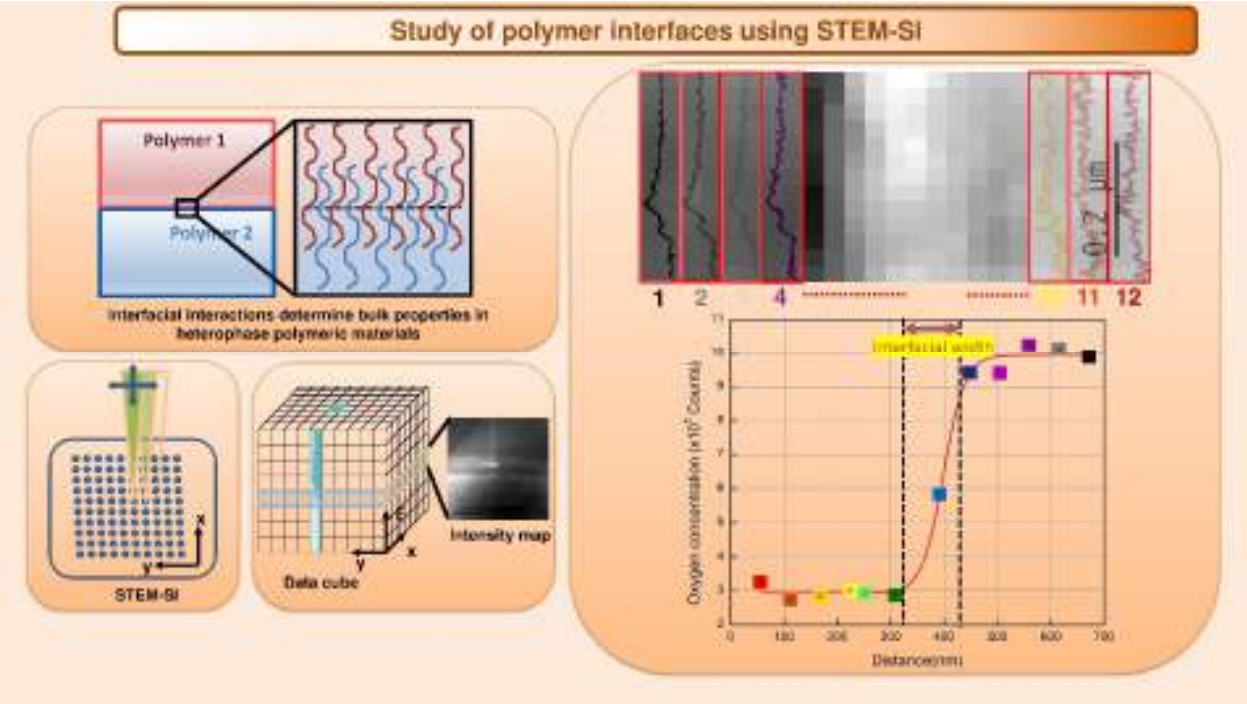

[1] Present Address: Department of Materials Science and Engineering, IIT Delhi, Delhi 110016, India

[2] Present Address: GSAIS, Kyoto University, 1 Yoshida-Nakaadachi-Cho, Sakyo-ku, Kyoto 606-8306, Japan

Abstract

Polymer blends are important for both commercial utility and scientific understanding. The degree of interfacial mixing in polymer blends, is important since it influences the blends' mechanical properties. Understanding bulk properties in multiphase polymeric materials requires knowledge of the interfacial properties in the materials. The characterization of interface, in terms of its width and composition profile, provides insight about the bulk behavior of the material. Chemical microscopy through electron energy-loss spectroscopy (EELS) in the transmission electron microscope (TEM) is gaining popularity to characterize narrow polymer-polymer interfaces. In this work, we show how STEM-SI (scanning TEM-spectrum imaging, a spatially resolved energy-loss spectroscopy) can be employed to calculate the interfacial width in a pair of immiscible polymers, taking a polycarbonate-polystyrene (PC-PS) bilayer as an example. By mapping peaks unique to each of the blend constituents at several points across the interface, we show how the interfacial profile concentrations can be determined. With this method we calculated the interfacial width in the PC-PS bilayer sample to be approximately 32 nm, even utilizing low resolution spectrometers, which are more widely available. Using the technique described with higher resolution EELS instruments having better signal-to-noise ratio, higher spatial resolution could be achieved. Using EELS chemical fingerprints of polymers that have been developed earlier, the technique presented here has the potential for effective visualization and morphological measurements of phase-differentiated polymer blends. This paper is an attempt to enable a new user to characterize polymer-polymer interfaces using chemical microscopy.

Keywords: Polymer interfaces, Spectrum imaging, STEM-SI, EELS

Introduction

Characterization of polymer-polymer interfaces, for measurement of properties such as interfacial width and composition profile, is important from both scientific and practical points of view. From the scientific viewpoint, the structure of the interface relates closely to the miscibility of two polymers, diffusion and wetting. From the industrial point of view, many polymer materials used as plastics, fibers or films involve one or more interfaces. Commercial polymeric materials have multicomponent structures, such as polymer blends, composites and laminates, where the bulk physical and mechanical properties are significantly affected by the structure and strength of interfaces.[1] The performances of coatings and adhesives correlate closely with the strength and durability of interfaces.[2] Often interfaces have complex morphology sometimes driven by equilibrium considerations specially in the case of block copolymers.

Measurement of interfacial properties is possible by several characterization techniques including but not limited to Rutherford backscattering (RBS),[3] Fourier-transform infrared spectroscopy (FTIR),[4] forward recoil spectrometry (FRES)[5] and nuclear reaction analysis (NRA).[6] Particularly for nanocharacterization, techniques such as ellipsometry,[7] neutron reflectometry[8] and secondary ion mass spectrometry (SIMS)[9] have been traditionally employed.

Ellipsometry is a relatively simple method that uses the change in polarization of light to determine the optical properties of the samples.[7,10] SIMS uses an ion beam to interact with a specimen and spectroscopically measure the ejected secondary ions. The mass/charge ratio of the outgoing secondary ions are analysed using a mass spectrometer to give information about elemental, isotopic and molecular composition of the surface.[11,12] Neutron reflectometry exploits the neutron refractive index (RI) profile normal to the reflection surface, where the RI depends on the atomic number as well as the isotope.[8] The technique provides a non-destructive method to

probe deeply buried interfaces and allows for in-situ measurements in different sample environments.[13] However, issues such as compositional profiling at the interface, morphological aspects of the interface and quantitative analysis are not provided by these techniques.[14] Furthermore, both ellipsometry and neutron reflectometry require optically flat samples from homogenous materials, with no impurities. Additionally, neutron scattering requires deuterated samples. Thus, commercial polymeric materials containing additives, do not suit well to be probed by the afore-mentioned techniques.

The need for a high spatial resolution technique without toxic preprocessing with real space observation has led to the adoption of electron energy-loss spectroscopy (EELS). EELS offers a unique advantage for investigation of polymeric interfaces in terms of the nano-scale spatial resolution. As compared to ellipsometry and neutron scattering, EELS has the advantage in sample preparation, by ultramicrotomy or cryo-ultramicrotomy and the ability to use heterogeneous industrial materials as samples.

The spectral signal from EELS represents the energy lost by electrons as they traverse through the thin TEM sample. The energy-specific energy-loss measured in EELS is a function of the chemical composition of the sample. A typical EELS spectrum can be broadly classified into three regions: Zero-loss peak (ZLP), low-loss region and core-loss edges. Each part of the spectrum can be used to extract different information such as dielectric properties, elemental composition, bonding and hybridization. A thorough review of EELS[15] has been reported recently and it can be referred for background information.

Scanning transmission electron microscopic - spectrum imaging (STEM-SI) combines the spatial resolution of a TEM with the chemical information provided by EELS. Within STEM-SI, a focused electron beam is raster scanned across the region of interest to collect energy-loss spectra

at each pixel (Figure 1a). The result is a spectrum image, which is a three-dimensional array representing spatial as well as spectral information. This is often referred to as a data cube as shown in Figure 1b.

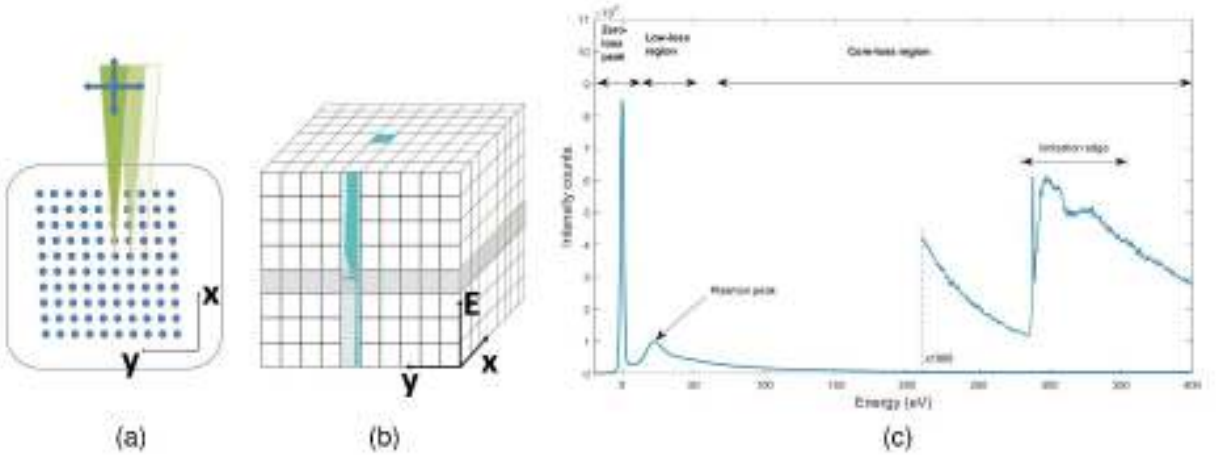

Figure 1: (a) Focused electron beam raster scan of STEM. (b) Data cube where EELS spectra are stored in each column (c) Typical EELS spectrum showing the zero-loss, low-loss and core-loss regions.

STEM-SI has been reported to measure interfacial properties, within polymer blends and substrate-adhesive interfaces. Studies on polystyrene/polyvinylpyridine (PS/PVP) blends have employed STEM-SI for determination of interfacial width.[16] The technique has been utilized to map the location of the modifier in a material.[17] The mechanism of interface formation between the surface of polybutylene terephthalate (PBT) sheet and an epoxy adhesive has been probed using STEM-SI.[18] The technique has also been used to measure the strength of silane-based epoxy adhesives used to bond aluminum structures.[19] The interface within polymeric biphasic nanoparticles has been characterized by the use of STEM-SI to gain insight into the nanocolloid morphology during synthesis.[20,21]

This paper outlines the use of STEM-SI to measure the interfacial width of unstained polycarbonate-polystyrene (PC-PS) bilayer. According to the author's knowledge, the interfacial

width in PC-PS blends has not been reported yet. The fraction of oxygen was measured as a function of position to identify, and subsequently characterize, the interface in an unstained PC-PS bilayer. Relative oxygen concentration was obtained by integrating the area under the core-loss edge. For absolute elemental quantification however, inelastic cross-section for the element is required. We could successfully characterize the interface without the need for use of heavy element staining.

Experimental

Polystyrene pellets were procured from Sigma-Aldrich with an average M_w of 350000 g/mol and a PDI of 2.06. The MFI was more than 1.3 g/10 min at 200°C under a load of 5 kg. Polycarbonate sheet, Lexan 101, was supplied by SABIC. From GPC, the M_w was estimated to be around 38892 g/mol with a PDI of 1.31. Its melt flow rate was 7 g/ 10 min at 300°C under a load of 1.2 kg. PC-PS bilayers were prepared by solvent casting a thick PS layer over a small piece of preformed PC sheet. A concentrated solution of PS in toluene was prepared by stirring PS pellets in the solvent overnight. Thus obtained clear solution was cast over a block of PC (3 mm thick and 1.5 cm in length). The block of PC was cut and trimmed with a razor blade in such a way that it could be used directly for ultramicrotomy after coating. The coated PC sample was air dried in a fume-hood for 24 hours. After drying, the sample was trimmed, also with a razor blade, to remove excess coating on other surfaces. Only the top surface coating was kept intact. Ultramicrotomy (Leica Ultracut UCT) of this sample was done such that the diamond knife cuts perpendicular to the interface formed within the bilayer sample. The sample thus obtained was used for STEM-SI experiments to measure the interfacial width.

A 200kV FEG-TEM (JEOL JEM 2100F) was used with Enfina EELS spectrometer whose energy resolution was 1.1 eV. The measurements were carried out at room temperature. There was

sufficient contrast in annular dark field images to identify the interfacial region (ROI) to be used for spectrum imaging. For each ROI, a pair of spectrum images were acquired, with different energy ranges. In each pair, the energy range of one SI focused on the low-loss region while the other focused on the oxygen K-edge at 532 eV. The SI was divided into equal regions across the interface. The spectral signals were extracted from each of the regions and routine spectra processing was performed involving background subtraction and correction for multiple scattering. The oxygen K-edge thus obtained for each region was used in interfacial width calculation.

STEM-SI was carried out by using the STEM mode in the electron microscope. As mentioned earlier, the STEM mode involves a focused electron probe which is able to raster scan across a specified region of interest (ROI). The electron beam was first aligned in STEM mode to get the required fine probe. High-angle annular dark field (HAADF) imaging was carried out within the STEM mode. Thus produced dark field image shows better contrast, in the unstained bilayer specimen, when compared to a bright field image. The HAADF imaging helped in selecting ROI at the interface. Furthermore, a small rectangular area across the interface was selected as the ROI. The ROI was divided into adequate number of pixels considering the trade-off between radiation damage and acquisition of strong signals. Energy dispersion was set at 0.5 eV/channel to maximize the signal. The beginning of the energy range was fixed as 400 eV. The combination of energy range and energy dispersion was such that it allowed the inclusion of oxygen edge at 532 eV along with sufficient energy range before the edge for background modelling and subtraction. The exposure time was 2 s/pixel. The electron dose was calculated to be at least 1-2 x 10^4 $e^-/Å^2$. The exposure time was drastically reduced to 10^{-6} s/pixel when spectrum image was acquired at the low-loss region (including the ZLP) due to high-intensity signal in this energy range.

Results

The PC-PS polymer pair shows a difference in their elemental composition, which was utilized in STEM-SI. EELS spectra taken from PC and PS are shown in Figure 2. The oxygen edge is visible in the energy-loss spectrum of PC, but it is absent in that of PS.

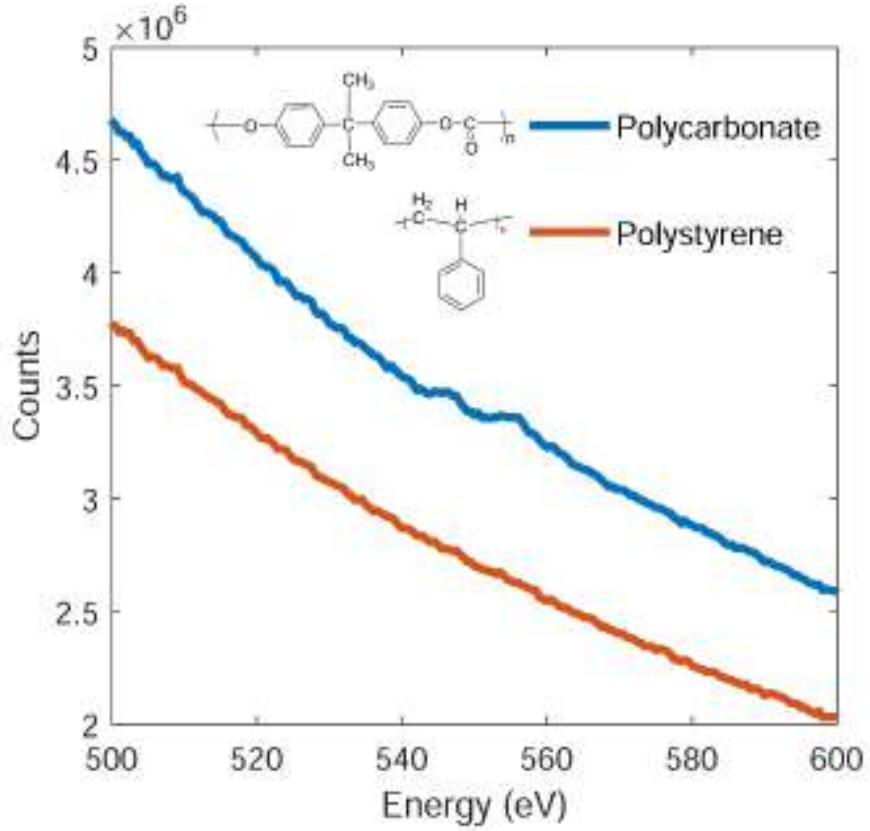

Figure 2: Core-loss region of PC and PS showing the difference in oxygen signal between the two polymers

At first, measurement was carried out at an original TEM magnification setting of 100,000X of which an area with 121 nm width and 319 nm length was used for spectrum-imaging. As presented in Figure 4, the area was divided into 11 x 29 pixels with a square pixel length of 11 nm. The ROI for the SI was selected across the interface and two spectrum-images were acquired over the same ROI. The energy range for the first SI included the oxygen edge at 532 eV. The energy range specified for second spectrum-image was limited to the low-loss region including the

zero-loss peak (ZLP). Since the signal in the low-loss region is high, exposure time per pixel was kept extremely low. The second spectrum-image was acquired to utilize the low-loss region for removal of multiple scattering effects at the oxygen K-edge. The resulting spectrum-image with typical extracted spectra in the low-loss region, oxygen core-loss region, and deconvolved oxygen K-edge, are shown in Figure 3.

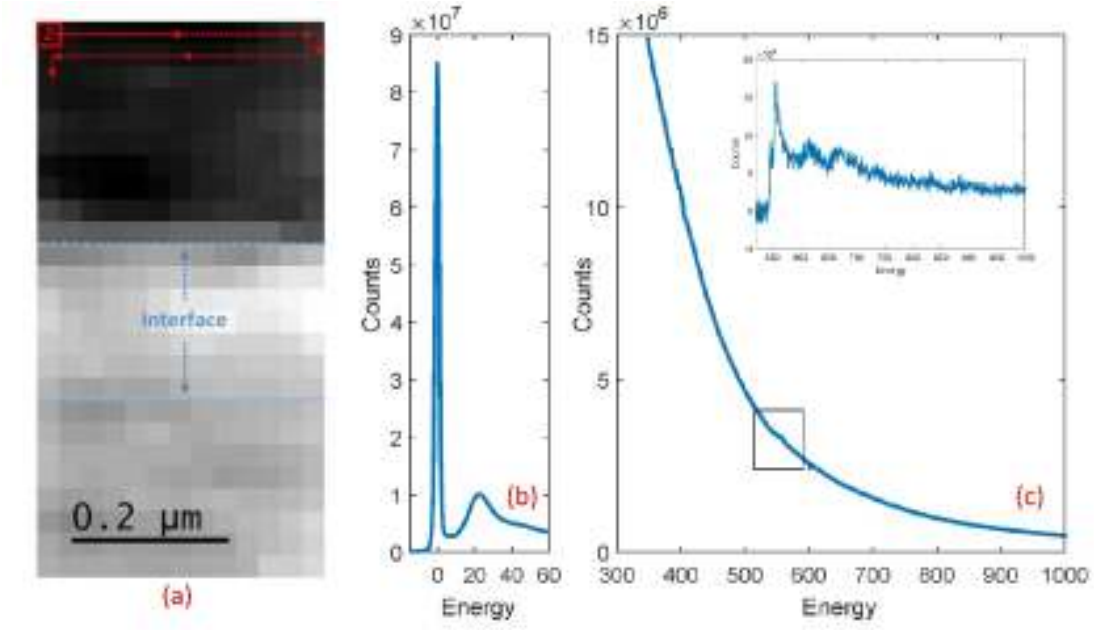

Figure 3: STEM-EELS Spectrum image along with typical extracted spectra. (a) SI showing a single pixel "z"(pixel dimensions here are 26.7 x 26.7 nm) and its raster scan path along with the interfacial region; (b) Typical low-loss spectrum extracted from a region of the SI and (c) Core-loss spectrum extracted showing presence of oxygen at 532 eV oxygen K-edge (Inset shows the deconvolved oxygen K-edge signal)

After SI acquisition, oxygen edge is extracted from regions of equal number of pixels running parallel to the interface (i.e. aligned along the interface) as can be seen in Figure 4(a). From each of these regions, the corresponding low-loss spectra were also extracted. The extracted signal is a sum of the signals from all the pixels within the region. The oxygen edge was

deconvolved after background subtraction (with the background modelled using a power-law function). The extracted oxygen edges from different regions are shown in Figure 4(b). It is evident from Figure 4(b), that the oxygen signal increases from one end of the ROI to the other, implying the presence of the interface within the ROI.

Subsequently, the integrated area under the oxygen edge within the energy range 530-560 eV (after background subtraction and deconvolution) was used as a proxy for concentration. The

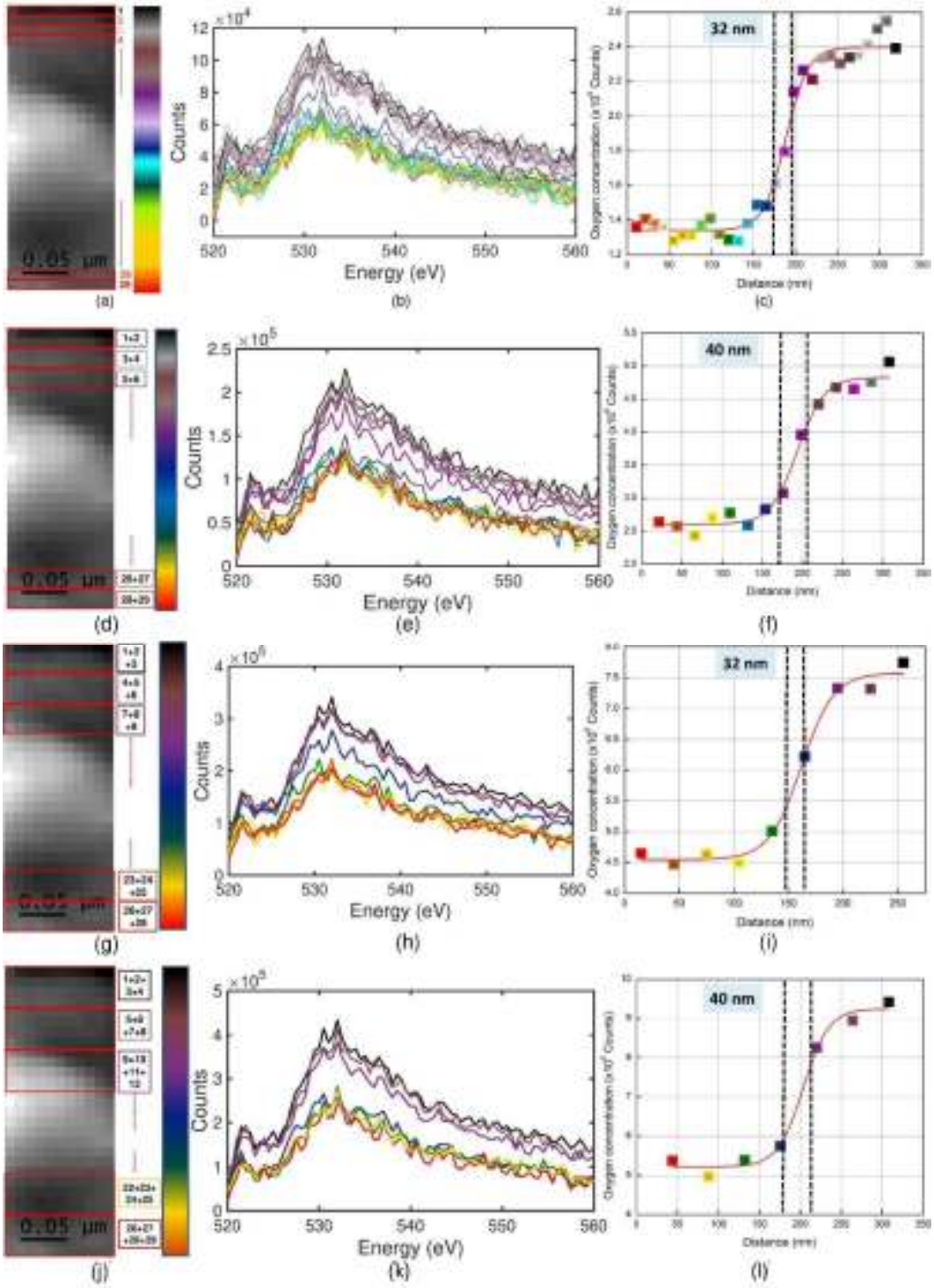

Figure 4: Spectrum Image (SI) at 100000X magnification showing the different ROIs, corresponding extracted oxygen signals and interfacial width calculation. The left panel (a,d,g,j) shows SI with ROIs of different sizes; The middle panel (b,e,h,k) shows superimposed oxygen K-edges (after background subtraction and deconvolution) extracted from the different ROIs of the SI; The right panel (c,f,i,l) shows a plot of integrated intensity of the oxygen edge and distance in the interface indicating the calculated interfacial width. Each region in left panel, its corresponding spectrum in the middle panel and subsequent intensity point in the right panel are indicated by the same color. Pixel dimensions are 11 x 11 nm.

Integrated intensity under the oxygen edge was calculated using a trapezoidal function. A plot of the integrated intensity (representing oxygen content) as a function of distance (calculated using pixel size in SI) was generated (Figure 4(c)). It was found that a sigmoidal function was able to fit the data. Equation 1 gives the Boltzmann's sigmoidal function used for data fitting.

$$y = \frac{A_1 - A_2}{1 + e^{(x-x_0)/dx}} - A_2$$

Where

A_1 = Initial value; A_2 = Final value; x_0 = Centre; dx = Time constant

The curve thus obtained was used to quantify the interfacial width by measuring the distance within which oxygen concentration varies. The two inflection points in the fitted sigmoidal curve were determined, the lower inflection point and the upper inflection point. In order to reduce the error arising from curve fitting, the lower inflection point was increased by ten percent and the upper inflection point was decreased by ten percent. Subsequently, the difference between the two inflection points gives the distance within which the oxygen concentration varies i.e. the interfacial width. The function has no physical meaning in terms of its use for the analysis. The interfacial width was calculated to be 32 nm. Similar calculations were also done by varying the number of pixels in the regions from which oxygen signal is extracted. Regions with the length of two-, three- and four-pixels were also taken to extract the oxygen signal. The resulting interfacial width is shown in Figure 4 (f) (i) and (l).

Further, lower spatial resolution measurements were carried out to check whether the decreased spatial resolution, with its advantage of lower beam damage, produces similar results for interfacial width measurement. An original TEM magnification of 40,000X was used out of which, an area of 347.1 nm width and 667.5 nm length was utilized for spectrum imaging. Figure 5 shows that the area for spectrum imaging was divided into 13 x 25 pixels with a square pixel

length of 26.7 nm. The resulting deconvolved oxygen K-edges are shown in Figure 5(b). Although there is significant noise, the signal is certainly high enough to differentiate the areas based on their oxygen content. The resulting plot of oxygen concentration (in terms of integrated intensity) with distance is shown in Figure 5(c). Similar to previous analysis, sigmoidal function was used to fit the data and interfacial width was calculated within 10% limits. Likewise, analysis was also done by varying the size of the regions from which oxygen signal is extracted. The results from smallest and largest region are presented in Figure 5. The interfacial width was determined to be 32 nm from this data. It is noticeable from the figure that a low spatial resolution during data collection may be sufficient to measure the interfacial thickness.

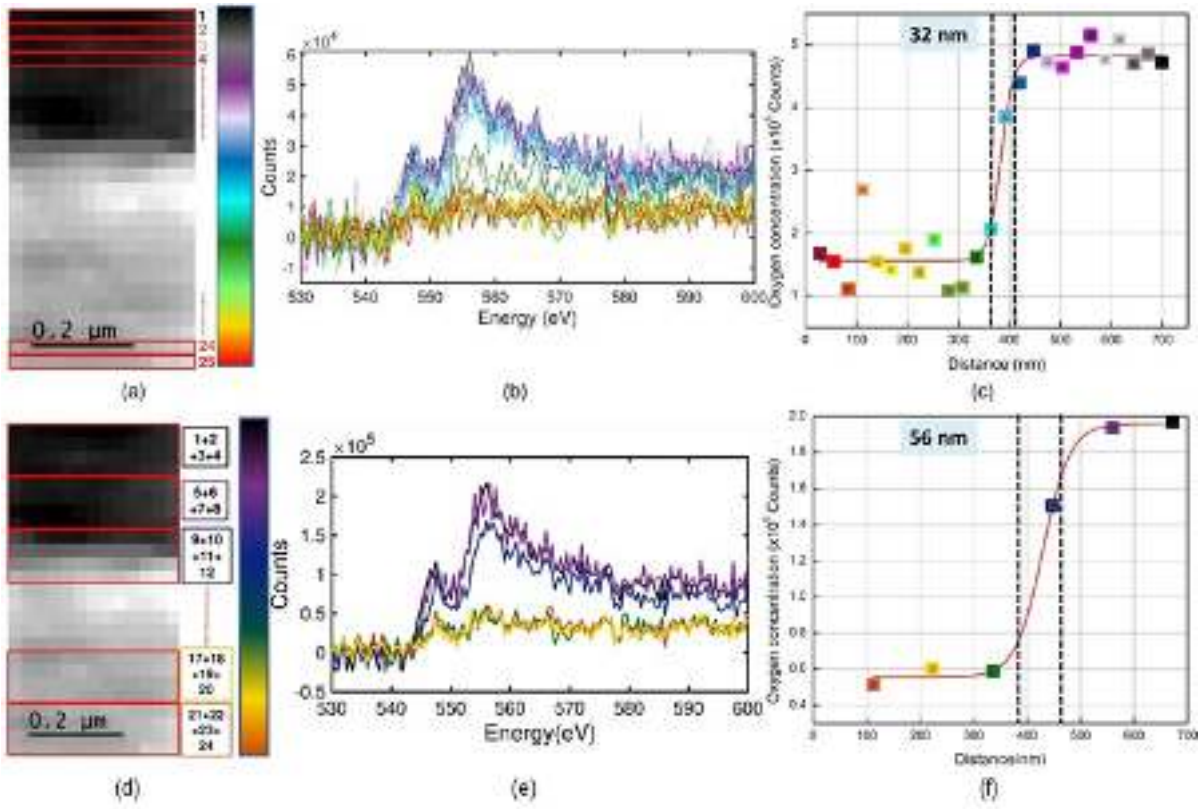

Figure 5: Spectrum Image (SI) at 40000X magnification showing the different ROI from which oxygen signals were extracted. The left panel (a,d) shows SI showing ROIs of different sizes; The middle panel (b,e) shows superimposed oxygen K-edges (after background subtraction and deconvolution) extracted from the different ROIs of the SI; The right panel (c,f) shows a plot of integrated intensity of the oxygen edge and distance in the interface indicating the calculated interfacial width. Each region in left panel, its corresponding spectrum in the middle panel and subsequent intensity point in the right panel are indicated by the same color. Pixel dimensions are 26.7 x 26.7 nm.

Radiation damage

Beam degradation is an inevitable part of analyzing polymeric systems using EELS. The image in Figure 6 were taken after spectrum-image acquisition. Prominent bright spots on a dark background are observed due to beam damage. The beam damage "spots" trace the movement of the focused electron beam during STEM-SI acquisition. The accuracy of width calculation improves as the number of pixels increase along with the exposure time per pixel, thereby increasing the overall SI acquisition time. Simultaneously, the radiation damage per pixel will drastically affect the quality of EELS signal acquired per pixel. Thus, the quality of SI (and consequently the data extracted from it) is not necessarily better when higher acquisition times are used. These effects can be reduced by using a cryo-holder. Perhaps radicals may diffuse across the sample and therefore cause interfacial width broadening. However, this effect has not been well studied since all the previous authors say that radicals are formed but are trapped.[22] But this should be studied further since it may affect interfacial width measurement and interface composition.

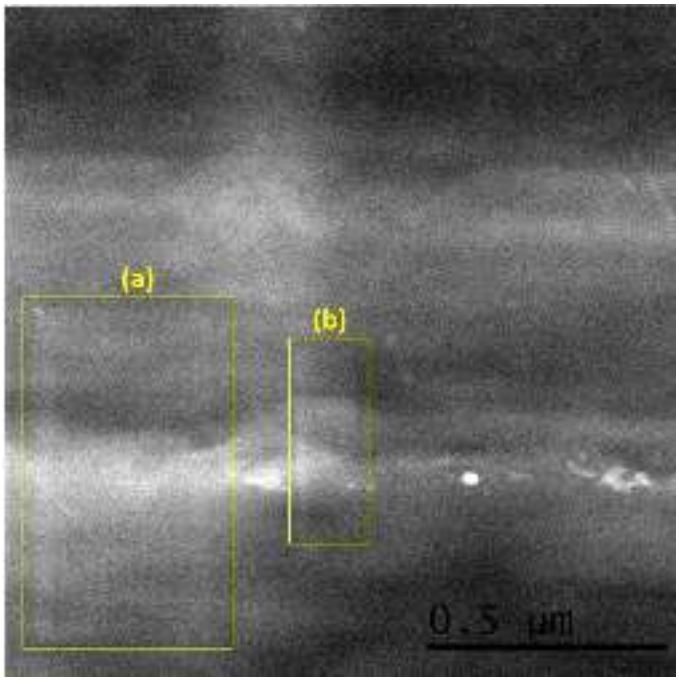

Figure 6: Annular dark field image showing the interface and the beam damage after SI acquisition. (a) Region taken for spectrum imaging at 40000X; (b) Region showing beam damage from SI at 100000X

At room temperature, in air or vacuum, PC predominantly undergoes chain scission and slight branching.[23] Although radiation damage of PC involves chain scission and formation of phenoxy and phenyl free radicals, [22–24] these radicals remain trapped within the sample at cryogenic temperatures. However, for non-cryogenic STEM-SI, the possibility of radicals diffusing away, escaping out of the sample and reacting with atoms further away cannot be ruled out. But ESR based measurements say the radicals decay with increasing temperature.[22] If the rates of diffusion are similar then the relative proportion of oxygen in the different polymers remains the same therefore not compromising the data potentially.

Discussion

Few important inferences can be made from Figures 4 and 5. Firstly, if the signal to noise ratio allows, the spectrum image should be divided into the smallest regions possible. At a fixed magnification, decreasing the area of spectral extraction, in a way, provides the maximum spatial resolution. Small areas allow for better visualization of the transition region for the energy-loss signal under consideration. Consequently, an accurate measurement of the interfacial width is possible. As seen from Figure 4(a), the least possible distance to be measured was 32 nm by summing the pixels from the smallest area selected. Secondly, carrying out the spectrum imaging at a higher magnification provides the actual increase in the spatial resolution, thereby resulting in a more accurate measurement of the interfacial width. The extraction of spectral data from regions of different sizes gives an interfacial width in the range of 32-40 nm, which is close to the values

suggested in literature for other immiscible polymer pairs determined by techniques other than STEM-SI. [7,14,18]

This study is an attempt to use STEM-EELS for interfacial width determination within a polymer bilayer. PC and PS are known to be incompatible and show partial miscibility.[25] On blending PC and PS, two different glass transition temperatures (T_gs) are observed, which implies that the polymers are miscible to a minor extent.[26] Their miscibility is affected by several factors such as processing technique, processing conditions as well as weight fraction.[26] Calculation of polymer-polymer interaction parameter also shows that PC and PS are partially miscible.[27] Thus, PC-PS blends/bilayers are expected to have a narrow interface.[25–27]

Particularly for immiscible polymer pairs such as PC-SAN and PMMA-SAN laminates, interfacial thickness has been reported to vary from 5-40 nm. These measurements have been done by EELS [14,18] as well as ellipsometry studies.[7] Our result of 32 nm wide interface is consistent with the expected thickness in such strongly segregated systems. However, there is the caveat that at high magnification, the low signal-to-noise ratio affects the accuracy of our measurement. Obtaining higher SNR at high magnification is important here which enables to detect small changes in concentration of oxygen over the spatial resolution of the interface.

Conclusion

In this study, we have elucidated the application of EELS through STEM-SI to the measurement of interfacial width in polycarbonate- polystyrene bilayers utilizing low energy resolution (~1.1 eV) analytical electron microscope. The difference in the presence of a heteroatom (here, oxygen) in the polymer structure was exploited to calculate the interfacial width. The width of the interface in the polymeric bilayer of PC and PS was found to be 32 nm. The accuracy of the

measurement depends on certain factors such as magnification, pixel size, acquisition time and averaging of pixels. However, radiation damage and weak EELS signal at high spatial resolution poses a limitation to the accuracy of interfacial width determination.

STEM-SI is one of the ways to utilize the spatial resolution provided by TEM towards chemical microscopy through energy-loss spectroscopy. The signal utilized in STEM-SI can range from a variety of spectral features such as low loss spectra, elemental edges and even chemical bonding peaks, if they are discernible enough. Chemical fingerprints of polymers can be exploited for chemical bond mapping in polymeric materials. An analytical TEM is a powerful tool for the study of nano-structured interfaces that require high spatial resolution alongside chemical information.

Acknowledgement

This work was carried out within the ARC Centre of Excellence in Exciton Science, supported by the Australian Research Council (ARC) via grant CE170100026. The authors acknowledge the use of the instruments and scientific and technical assistance of Prof. Laure Bourgeois, Prof. Matthew Weyland and Dr. Emily Chen at the Monash Centre for Electron Microscopy, a Node of Microscopy Australia. This research used equipment funded by the Australian Research Council grant LE0454166. The authors also acknowledge IITB-Monash Research Academy and Central facilities (Cryo-HRTEM), IIT Bombay, for their support and co-operation and SABIC for industrial sponsorship. R.P. thanks Asst. Prof. Tushar Gupta (National Institute of Technology Rourkela, India) for support in data processing and data representation within the manuscript.

References

1. Fredrickson GH. *Phys Polym Surfaces Interfaces*. 1992;1–28.
2. Horiuchi S, Yin D, Ougizawa T. *Macromol Chem Phys*. 2005;**206**:725–31.
3. Composto RJ, Kramer EJ. *J Mater Sci*. 1991;**26**:2815–22.
4. Alsten JG Van, Lustig SR. *Macromolecules*. 1992;**25**:5069–73.
5. Nealey PF, Cohen RE, Argon AS. *Macromolecules*. 1993;**26**:1287–92.
6. Shearmur TE, Clough AS, Drew DW, Van Der Grinten MGD, Jones RAL. *Macromolecules*. 1996;**29**:7269–75.
7. Yukioka S, Inoue T. *Polymer (Guildf)*. 1993;**34**:1256–9.
8. Fernandez ML, Higgins JS, Penfold J, Ward RC, Shackleton C, Walsh DJ. *Polymer (Guildf)*. 1988;**29**:1923–8.
9. Davies MC, Lynn RAP. *Clin Mater*. 1990;**5**:97–114.
10. Higashida N, Kressler J, Satoshi Y, Inoue T. *Macromolecules*. 1992;**25**:5259–62.
11. Leeson AM, Alexander MR, Short RD, Briggs D, Hearn MJ. *Surf Interface Anal*. 1997;**25**:261–74.
12. Chan CM, Weng LT, Lau YTR. *Rev Anal Chem*. 2014;**33**:11–30.
13. Torikai N, Yamada NL, Noro A, Harada M, Kawaguchi D, Takano A, et al. *Polym J*. 2007;**39**:1238–46.
14. Horiuchi S, Hanada T, Yase K, Ougizawa T. *Macromolecules*. 1999;**32**:1312–4.
15. Pal R, Sikder AK, Saito K, Funston AM, Bellare JR. *Polym Chem*. 2017;6927–37.
16. Siangchaew K, Libera M. *Macromolecules*. 1999;**32**:3051–6.
17. Tremblay A, Tremblay S, Favis BD, Selmani A, Lesperance G. *Macromolecules*. 1995;**28**:4771–3.
18. Horiuchi S, Hamanaka T, Aoki T, Miyakawa T, Narita R. *J Electron Microsc (Tokyo)*.

2003;**52**:255–66.

19. Bertho J, Stolojan V, Abel M-L, Watts JF. *Micron*. 2010;**41**:130–4.

20. Kim G, Meyers D. *Microsc Microanal*. 2009;**15**:484.

21. Kim G, Sousa A, Meyers D, Libera M. *Microsc Microanal*. 2008;**14**:459–68.

22. Babanalbandi A, Hill DJT, Whittaker AK. *Polym Adv Technol*. 1998;**9**:62–74.

23. Davis A, Golden JH. *J Macromol Sci Part C*. 1969;**3**:49–68.

24. Hareesh K, Sanjeev G. In: Springer Series on Polymer and Composite Materials. 2019. p. 138–58.

25. Kim WN, Burns CM. *J Appl Polym Sci*. 1987;**34**:945–67.

26. Chuai CZ, Almdal K, Johannsen I, Lyngaae-Jorgensen J. *Polym Eng Sci*. 2002;**42**:961–8.

27. Scott RL. *J Chem Phys*. 1949;**17**:279–84.